Investigating the regulatory mechanism of glucose metabolism by ubiquitin-like protein MNSFβ

Megumi Kono[1], Kyoko Yamasaki[1], Morihiko Nakamura[1]

Author information

Megumi Kono[1]
mkono8@med.shimane-u.ac.jp

Kyoko Yamasaki[1]
kyoko731@med.shimane-u.ac.jp

Morihiko Nakamura[1]
nkmr0515@med.shimane-u.ac.jp

Affiliations
1 The Department of Cooperative Medical Research. Office for Regional Collaboration and Innovation, Shimane University, Izumo, Japan

Address for correspondence: Professor Morihiko Nakamura, Department of Cooperative Medical Research, Head Office for Regional Collaboration and Innovation, Shimane University, 89-1 Enya-Cho, Izumo 693-8501, Shimane, Japan. Tel.: +81-853-20-2916; Fax: +81-853-20-2913; Email: nkmr0515@med.shimane-u.ac.jp

ORCID: https://orcid.org/0000-0003-1079-9787

Abstract

Background: Monoclonal nonspecific suppressor factor β (MNSFβ), a ubiquitously expressed member of the ubiquitin-like protein family, is associated with diverse cell regulatory functions. It has been implicated in glycolysis regulation and cell proliferation enhancement in the macrophage-like cell line Raw264.7. This study aims to show that HIF-1α regulates MNSFβ-mediated metabolic reprogramming.

Methods and results: In Raw264.7 cells, MNSFβ siRNA increased the oxygen consumption rate and reactive oxygen species (ROS) production but decreased ATP levels. Cells with MNSFβ knockdown showed a markedly increased ATP reduction rate upon the addition of oligomycin, a mitochondrial ATP synthase inhibitor. In addition, MNSFβ siRNA decreased the expression levels of mRNA and protein of HIF-1α—a regulator of glucose metabolism. Evaluation of the effect of MNSFβ on glucose metabolism in murine peritoneal macrophages revealed no changes in lactate production, glucose consumption, or ROS production.

Conclusion: MNSFβ affects both glycolysis and mitochondrial metabolism, suggesting HIF-1α involvement in the MNSFβ-regulated glucose metabolism in Raw264.7 cells.

Keywords: Ubiquitin-like protein MNSFβ, HIF-1α, Metabolism, Metabolic reprogramming

Abbreviations

CBP	CREB-binding protein
C-TAD	carboxy-terminal transactivation domain
FIH	factor-inhibiting HIF-1α
HIF-1	hypoxia-inducible factor-1
IFNγ	interferon γ
LPS	lipopolysaccharide
MNSFβ	monoclonal nonspecific suppressor factor β
NF-κB	nuclear factor-kappa B
OCR	oxygen consumption rate
ODDD	oxygen-dependent degradation domain
OXPHOS	oxidative phosphorylation
PDK1	Pyruvate dehydrogenase kinase 1
PHD	prolyl hydroxylase
pVHL	von Hippel Lindau protein
ROS	reactive oxygen species
TCA	tricarboxylic acid
2-DG	2-deoxy-D-glucose

Introduction

Monoclonal nonspecific suppressor factor β (MNSFβ), a member of the ubiquitin-like protein family, is involved in various biological functions, such as cell proliferation, immunological responses, and apoptosis. MNSFβ presents a 57% amino acid sequence homology and 36% similarity with ubiquitin [1]. The C-terminal glycine doublet of ubiquitin, which participates in the isopeptide bond formation during conjugation, is a conserved sequence even in MNSFβ [2]. MNSFβ forms covalent bonds with certain lysines of specific target proteins, including endophilin II and Bcl-G. While MNSFβ covalently attaches to endophilin II and downregulates phagocytosis in macrophages [3,4], it also covalently binds to Bcl-G and markedly promotes apoptosis induced by lipopolysaccharide (LPS)/interferon γ (IFNγ) in macrophages [5]. Unlike ubiquitin, MNSFβ may not be involved in the degradation of targeted proteins. While MNSFβ regulates glycolysis, its effects is related to GLUT1 [6]. Hypoxia-inducible factor-1α (HIF-1α) controls GLUT1 expression in multiple cell lines, but whether MNSFβ affects HIF-1α remains unclear.

The heterodimeric transcription factor HIF-1 increases the expression of enzymes implicated in glucose metabolism, such as hexokinase, phosphofructokinase-1, and pyruvate kinase M2 [7]. HIF-1 comprises two subunits: an oxygen-labile HIF-1α subunit and a constitutively stable HIF-1β subunit. HIF-1α has an oxygen-dependent degradation domain (ODDD) that binds the E3 ubiquitin ligase von Hippel Lindau protein (pVHL). Prolyl hydroxylases (PHDs) hydroxylate the two proline residues (Pro^{402}, Pro^{564}) within the ODDD, which recruits pVHL, and HIF-1α is ubiquitinated and degraded by the 26S proteasome. In hypoxia, PHD inhibition impedes pVHL binding. This is followed by HIF-1α stabilization, nuclear translocation, dimerization with HIF-1β, coactivator recruitment, and binding to hypoxia response elements in the promoter region of target genes [7,8]. The asparaginyl hydroxylase factor-inhibiting HIF-1α (FIH) suppresses HIF-1α transcriptional activity. FIH causes hydroxylation of HIF-1α at the Asn^{803} in the carboxy-terminal transactivation domain (C-TAD), which prevents HIF-1α binding to transcriptional coactivators, such as CREB-binding protein (CBP)/p300 [9]. FIH overexpression suppresses HIF-1α transcriptional activity [10]. The histone acetyltransferase CBP/p300 are relevant to HIF-1α/β heterodimer formation. Acetylated CBP/p300 interacts with the C-TAD of HIF-1α to enhance gene expression [8]. Certain cancer cells showed overexpressed CBP/p300 mRNAs [11]. Hypoxia, alongside many oncogenic and inflammatory stimuli, promotes HIF-1α activation and accumulation [12,13]. HIF-1α overexpression has been found in various cancer types and is related to tumor aggressiveness [13-15].

In this study, MNSFβ alters both glycolysis and mitochondrial metabolism, markedly affecting glucose metabolism and cytokine production, and HIF-1α may be involved in this regulatory mechanism.

Materials and methods

Antibodies and chemicals

Antibodies used included anti-HIF-1α (Novus Biologicals, Littleton, CO, USA), anti-Acetyl-CBP (Lys1535)/p300 (Lys1499) (Cell Signaling Technology, Beverly, MA, USA), anti-FIH (Cell Signaling Technology), anti-PHD2 (GeneTex, San Antonio, TX), anti-β-actin (Medical & Biological laboratories), and peroxidase-conjugated rabbit immunoglobulin G antibody (Cappel, Solon, OH, USA). Sigma (St. Louis, MO, USA) supplied LPS and oligomycin A.

Cell culture, siRNAs, and transfection of cells

The macrophage-like cell line Raw264.7 was obtained from ATCC (Manassas, VA). Cells were maintained in Dulbecco's modified Eagle's medium containing 10% fetal bovine serum and penicillin/streptomycin (1:100). siRNAs were purchased from Qiagen (Chatsworth, CA, USA). The target sequence of siRNAs was as follows: MNSFβ 5′-CCACCCTGCCATGCTAATAAA-3′ and the scrambled negative control 5′-AATTCTCCGAACGTGTCACGT-3′. siRNA transfection was performed with HiPerFect Transfection Reagent (Qiagen) following the manufacturer's instructions.

cDNAs and transfection cells

cDNAs were prepared as previously described [2]. cDNA encoding MNSFβ was subcloned into the vector pcDNA3.1(+) (Invitrogen). DNA transfection was performed using Lipofectamine LTX reagent with Plus reagent (Invitrogen), following the manufacturer's instructions. Cells were seeded and cultured until 70%–80% confluent. Lipofectamine LTX and Plus reagent was mixed with cDNA. The DNA mixture was incubated for 5 min at room temperature to form a DNA-lipid complex and added to cells. The final volume of cDNA was 500 ng per well.

Western blotting

Protein samples were subjected to SDS-PAGE and electro-transferred from gels to polyvinylidene fluoride membranes. Membranes were blocked for 1 h at room temperature using Tris-buffered saline with 0.02% Tween 20 (TBST) and 5% skim milk or 5% bovine serum albumin and probed with primary antibodies overnight at 4 ℃ in blocking buffer. The membranes were washed four times for 5 min each with TBST and incubated with horseradish peroxidase secondary antibodies for 2 h at room temperature. The secondary antibodies were used at 1:15000 dilutions in blocking buffer. Membranes were washed four times for 5 min each with TBST and detected with enhanced chemiluminescence reagents (Amersham Biosciences) and analyzed with ImageJ software.

Reverse transcription polymerase chain reaction (RT-PCR)

RT-PCR was performed with Premix Taq (Ex Taq Version 2.0) (Takara) following the manufacturer's instructions. The PCR conditions used were as follows: initial denaturation at 95 ℃ for 1 min, 40

cycles of 98 ℃ for 10 s, 55 ℃ for 30 s, and 72 ℃ for 1 min. Primers for HIF-1α were 5′-TGATGTGGGTGCTGGTGTC-3′ (sense) and 5′-TTGTGTTGGGGCAGTACTG-3′ (anti-sense). Primers for GAPDH were 5′-CAACTACATGGTTTACATGTTC-3′ (sense) and 5′-GCCAGTGGACTCCACGAC-3′ (anti-sense). We amplified GAPDH as an internal standard. PCR products were electrophoresed on 2% agarose gels with ethidium bromide and detected using ultraviolet (UV) transilluminator. The signals were quantified with ImageJ software.

Reactive oxygen species (ROS) detection

Cells were seeded at 2.0×10^4 cells per well in a 96-well black microplate. Intracellular ROS was evaluated with a ROS Assay Kit-Highly sensitive DCFH-DA- (Dojindo) according to the manufacturer's instructions. Loading buffer (10×) was diluted with double-deionized water, and highly sensitive DCFH-DA was diluted with loading buffer to prepare the working solution. Cells were washed twice using Hanks' Balanced Salt Solution (HBSS) (Sigma), and incubated with the highly sensitive DCFH-DA dye working solution at 37 ℃ for 30 min in the dark. Cells were washed twice, and each well was refilled with HBSS. Fluorescence was read using a microplate reader (Beckman Coulter). Excitation and emission wavelengths were set at 485 and 535 nm, respectively.

Electrophoretic mobility shift assay (EMSA)

Cells were seeded at 1.0×10^6 cells per well in a 6-well plate. Nuclear extracts were prepared with EzSubcell Fraction (ATTO) according to the manufacturer's instructions. HIF-1α binds to hypoxia response element (HRE) sequences within the promoter region. HIF-1α-DNA interactions were detected using biotin end-labeled DNA probes containing HRE. The sequence of the probe was 5′-CACCCCACCCCCGTGAGGAGGAGGGTGAGGAAAC-3′. The binding reaction was performed using a Gelshift Chemiluminescent EMSA kit (Active Motif) following the manufacturer's instructions. The reaction products were loaded on a 6% polyacrylamide gel in 0.5% Tris borate/EDTA at 4 ℃, transferred to a nylon membrane, and fixed on the membrane by UV cross-linking. The biotin-labeled probe was detected using chemiluminescence.

ATP measurement

Cells were seeded at 1.0×10^4 cells per well in a 96-well white microplate. Intracellular ATP was detected using an ATP Assay Kit-Luminescence (Dojindo) according to the manufacturer's instructions. Substrate (firefly luciferin) was dissolved in assay buffer supplied by the manufacturer. The solution was added to the enzyme solution to obtain working solution. The culture medium was removed from the wells and cells were incubated with 100 µl of working solution at 25 ℃ for 10 min. Luminescence was read with a microplate reader at 556 nm (Promega). The ATP concentrations were calculated from a calibration curve generated from the ATP standard; ATP measurement had a

detection limit of 0.05 µmol/l ATP.

OCR detection

Cells were seeded at 1.0×10^4 cells per well in a 96-well black microplate. The mitochondrial oxygen consumption rate (OCR) was evaluated using an Extracellular OCR Plate Assay Kit (Dojindo) based on the manufacturer's instructions. Oxygen probe was diluted with medium to prepare the working solution. The culture medium was removed from the wells and cells were incubated with 100 µl of working solution at 37 ℃ for 30 min in a microplate reader. Then, one drop of mineral oil was added to each well, and the cells were incubated at 37 ℃ for 5 min. Fluorescence was read using a microplate reader at 10-min intervals for 200 min. Excitation and emission wavelengths were set at 500 and 660 nm, respectively. The OCR (pmol/min) was calculated from the intensity using the calculation sheet provided by the manufacturer.

Glucose and lactate assay

Peritoneal macrophages were seeded at 2.0×10^5 cells per well in a 24-well plate. Glucose and lactate in the supernatant were detected using a glucose assay kit-WST (Dojindo) and glycolysis cell-based assay kit (Cayman) based on the manufacturer's instructions, respectively. The concentrations were calculated from a calibration curve generated from the standard. The glucose assay had a detection limit of 0.02 mmol/l glucose.

Proteome profiler mouse cytokine array

Cells were seeded at 1.0×10^5 cells per well in a 24-well plate. The cytokine expressions in cell culture supernatants were detected using a Proteome Profiler Mouse Cytokine Array Kit, Panel A (R&D Systems) following the manufacturer's instructions. Cell culture supernatants were cleared of particulates by centrifugation for 5 min at 1,000 ×g and then used for the cytokine array. The signal was quantified using ImageJ software.

Metabolome analysis

The cells were washed with phosphate buffered saline and lysed using 70% (v/v) methanol. Metabolome analysis by gas chromatography-mass spectrometry (GC/MS) was performed at the Integrated Center for Mass Spectrometry, Graduate School of Medicine, Kobe University.

Isolation of peritoneal macrophages

Peritoneal macrophages were harvested from female BALB/c mice (Japan SLC, Inc.) 4 days after intraperitoneal injection of 1.5 ml of sterile 4% Brewer's thioglycollate medium (Difco Laboratories). The cells were collected by centrifugation at 400 ×g for 5 min, washed and seeded in Dulbecco's

modified Eagle's medium supplemented with 10% fetal bovine serum. The collected macrophages were used in various experiments, including western blotting and ROS assay. Peritoneal macrophages (1.0×10^5 cells per well) were transfected with siRNAs for 48 h, and HIF-1α expression was detected using anti-HIF-1α antibody. Collected macrophages were seeded at 2.0×10^4 cells in ROS assay. After 48-h transfection of MNSFβ siRNA, intracellular ROS was evaluated. All experiments with animals in this study were approved by the Animal Care and Use Committee of Shimane University.

Statistical analysis

Statistical significance was analyzed by Student's t-test and expressed as *P* values. $p < 0.05$ was considered statistically significant.

Results

MNSFβ siRNA increased oxidative phosphorylation in Raw264.7 cells

We most recently reported that MNSFβ regulates the glycolytic system [6]. Mitochondrial respiration is closely involved in the mechanism of intracellular glycometabolism. For instance, glycolytic suppression enhances mitochondrial oxidative phosphorylation (OXPHOS) [16,17]. Thus, we examined the effect of MNSFβ on metabolism in mitochondria. As depicted in Fig. 1a (upper panel), MNSFβ siRNA strongly knocked down the expression of MNSFβ. First, we determined whether glycolytic suppression induced by MNSFβ siRNA affects OXPHOS in Raw264.7 cells. We next measured the OCR, an indicator of metabolic activity in mitochondria, and ROS, a byproduct of oxidative phosphorylation. After 48 h transfection, MNSFβ siRNA significantly increased both OCR and ROS production in Raw264.7 cells (Fig. 1a, 1b). Conversely, 18 h of MNSFβ overexpression reduced ROS production, strongly indicating that this ubiquitin-like protein positively regulates ROS production (Fig. 1c). In addition, we measured ATP levels in Raw264.7 cells transfected with MNSFβ siRNA and treated with the ATP synthase inhibitor oligomycin. MNSFβ siRNA transfection markedly reduced ATP levels. Upon oligomycin treatment, cells with MNSFβ knockdown exhibited a greater ATP reduction rate than the controls (Fig. 1d), suggesting that MNSFβ siRNA treatment may alter the main ATP source from glycolysis to OXPHOS.

MNSFβ affects HIF-1α expression and HIF-1α–DNA interactions in Raw264.7 cells

In macrophages, HIF-1α disruption facilitates OXPHOS and decreases the glycolysis level [18]. MNSFβ siRNA can inhibit the expression of GLUT1, GLUT3, and the key molecules in glycolysis [6]. HIF-1α enhances glycolysis by inducing the expression of glycolytic enzymes and glucose transporters. To examine whether HIF-1α mediates MNSFβ-regulated glycolysis, we analyzed the expression of mRNA and protein of HIF-1α. After 48 h transfection of MNSFβ siRNA, HIF-1α mRNA and protein expressions were significantly decreased (Fig. 2a). Evaluation of t

he DNA binding property of HIF-1α by EMSA revealed that MNSFβ siRNA impaired DNA–HIF-1α interaction (Fig. 2b). These results strongly indicate that MNSFβ knockdown-triggered reduction in HIF-1α transcriptional activity may be implicated in glycolysis suppression.

MNSFβ siRNA decreases acetyl-CBP/p300 expression in Raw264.7 cells

The stability and transcriptional activity of HIF-1α are regulated by its post-translational modifications such as ubiquitination, hydroxylation, and acetylation [7]. Therefore, we examined whether MNSFβ affects factors involved in HIF-1α stabilization and complex formation. After 48 h transfection, MNSFβ siRNA reduced acetyl-CBP/p300 expression (Fig. 3a) without altering that of FIH and PHD2 (Fig. 3b, 3c). These results indicate that MNSFβ siRNA-induced decrease in HIF-1α transcriptional activity is affected not only by HIF-1α but also by decreased expression of acetyl-CBP/p300, which suppresses glycolysis through decreased expression of HIF-1α target genes.

MNSFβ siRNA changes intracellular metabolite levels in Raw264.7 cells

In cancer cells, HIF-1α activation diminishes the tricarboxylic acid (TCA) cycle and OXPHOS [19,20]. To investigate further MNSFβ knockdown-triggered glycolytic changes, intermediate metabolites were detected by GC-MS. After 48 h transfection, MNSFβ siRNA reduced pyruvate and lactate, TCA cycle intermediates, especially citrate (Table 1). Among the amino acids, proline and branched chain amino acids were greatly reduced, while only serine was increased. These data suggest that MNSFβ affects overall glucose metabolism and partially alters amino acid metabolism as well.

MNSFβ changes the pattern of cytokine production in Raw264.7 cells

HIF-1α can alter cytokine expression, which markedly contributes to the tumor microenvironment [21,22]. Metabolites can affect cytokine production [23]. Since MNSFβ knockdown altered HIF-1α expression as described above, we investigated the relationship between MNSFβ and cytokine expression. After 48 h transfection, the cells were treated with 1 μg/ml LPS for 24 h, and cytokines in the supernatants were analyzed by antibody arrays, resulting in 16 cytokines (Fig. 4). Among them, CCL2 and IL-10 were reported to be decreased by HIF-1α inhibition [24]. ICAM-1 is related to HIF-1α and GLUT1 expression during endotoxemia [25]. Thus, MNSFβ may modulate its effects on cytokine expression via HIF-1α.

MNSFβ affects HIF-1α expression in peritoneal macrophages

To further investigate the effect of MNSFβ on glucose metabolism, murine peritoneal macrophages were used. MNSFβ knockdown decreased HIF-1α mRNA (Fig. 5a). Unlike Raw264 cells, in unstimulated peritoneal macrophages, the expression level of HIF-1α protein is very low [26]. However, since the expression of HIF-1α protein is increased by LPS stimulation [26], we examined

the effect of MNSFβ on HIF-1α expression in LPS-stimulated murine peritoneal macrophages. MNSFβ knockdown markedly inhibited LPS-stimulated increase in HIF-1α protein expression (Fig. 5b). Since our previous study showed glucose consumption and lactate secretion by MNSFβ knockdown in Raw264.7 cells [6], we performed the same verification in peritoneal macrophages. Unlike Raw264.7 cells, peritoneal macrophages treated with MNSFβ siRNA showed no difference in glucose and lactate levels in the culture supernatant or in ROS production (Fig. 5c, 5d, and 5e).

Discussion

In macrophages, metabolic characteristics are closely related to phenotypes and functions [27]. MNSFβ is involved in glycolytic regulation [6]. Therefore, in this study, we first focused on metabolic changes in mitochondria. MNSFβ knockdown increased OCR and ROS production in Raw264.7 cells (Fig. 1a, 1b), which showed a markedly decreased ATP level upon oligomycin treatment (Fig. 1d). In addition, MNSFβ siRNA reduces lactate in the culture supernatant and glucose consumption in Raw264.7 cells [6], suggesting that MNSFβ knockdown shifts the primary ATP production pathway from glycolysis to OXPHOS.

Many cancer cells rely on the glycolytic system for much of their ATP production, even though mitochondrial function is maintained under aerobic conditions [28]. This phenomenon is widely known as the Warburg effect, in which HIF-1α is closely involved [29]. HIF-1α promotes the glycolytic system and causes metabolic reprogramming by inhibiting pyruvate influx into the TCA cycle and OXPHOS [19]. Pyruvate dehydrogenase kinase 1 (PDK1) is a particularly important enzyme in the metabolic shift from mitochondria to the glycolytic system, and *PDK1* is a target gene of HIF-1α. Increased PDK1 by HIF-1α activation inhibits pyruvate dehydrogenase (PDH), thereby reducing mitochondrial respiration and ROS production and preventing cell death due to excess ROS [20,30]. Thus, the results shown in Fig. 1 are consistent with reports that MNSFβ knockdown reduces PDK1 expression [6].

HIF-1α and autoacetylation activate CBP/p300, which is involved in various gene expression [31]. MNSFβ siRNA decreased HIF-1α expression and transcriptional activity (Fig. 2) and acetyl-CBP/p300 expression (Fig. 3a). The decreased HIF-1α transcriptional activity probably resulted from decreased HIF-1α and acetyl-CBP/p300 expression. It is improbable that MNSFβ is involved in protein degradation, as previously reported [32]. CBP/p300, which binds to HIF-1α, is a histone acetylase that acetylates DNA. It reduces the binding between histones and DNA as well as the recruiting transcription factors and binding sites. Therefore, the decrease in acetyl-CBP/p300 may inhibit the binding of HIF-1α to DNA. Further experiments are needed to determine how MNSFβ affects HIF-1α and acetyl-CBP/p300 expression.

The TCA cycle is indirectly involved in energy production by producing NADH and FADH2 for transfer to the electron transport chain. In addition, TCA cycle metabolites become building

biomolecules or participate in chromatin modification and post-translational protein modifications [33,34]. HIF-1α activation suppresses the influx of pyruvate into the TCA cycle, but TCA cycle intermediates in the TCA cycle are compensated for by other metabolic pathways [35]. The results of reduced lactate and pyruvate in Raw264.7 cells with MNSFβ knockdown in metabolomic analysis corroborate our previous findings [6]. In addition, TCA cycle intermediates, especially citrate, were decreased, possibly due to glycolytic inhibition in MNSFβ-knockdown cells.

Metabolic reprogramming markedly contributes to the adaptive immune response by affecting cytokine secretion. LPS-stimulated macrophages enhance glycolysis, the pentose phosphate pathway, and fatty acid synthesis via the activation of transcription factors such as HIF-1α and STAT1/3 [23,36]. In human monocyte-derived macrophages, LPS promotes the secretion of pro-inflammatory cytokines mediated by Akt kinases. This is inhibited by the glycolytic inhibitor 2-deoxy-D-glucose (2-DG) [37]. In a mouse model of inflammatory disease induced by LPS administration, 2-DG also inhibits the secretion of cytokines such as IL-6, IL-1β, and TNFα, reducing inflammatory symptoms in mice [38]. In murine myeloid leukemia cells, nuclear factor-kappa B (NF-κB) binds to the promoter region of IL-6 and promotes IL-6 production [39]. MNSFβ knockdown markedly promotes LPS-induced degradation of IκBα, as we have reported [32]. Therefore, this suggests NF-κB involvement in the MNSFβ knockdown-triggered increase in IL-6.

Zhen XX *et al.* reported that MNSFβ knockdown decreased TNF-α mRNA expression in the human monocyte cell line Thp1-derived macrophages stimulated with LPS for 1 h or 4 h [40]. However, in murine macrophage Raw264.7 cells stimulated with 100 ng/ml LPS for 4 h, MNSFβ knockdown increased TNFα in the culture supernatant [41]. The effect of MNSFβ on LPS-induced TNF-α production appears to vary by cell type and stimulation conditions.

IL-1ra, an anti-inflammatory cytokine and IL-1 receptor antagonist, competitively inhibits IL-1α and IL-1β signaling. In Raw264.7, increased IL-1ra secretion by LPS is mediated by P2X7 receptor (P2X7R) activation [42]. P2X7R is a receptor whose ligand is extracellular ATP, which is abundantly expressed in immune cells. Extracellular ATP release is increased by stimulation of ROS, nitric oxide, TLR2, and TLR4 [43]. MNSFβ knockdown increased ROS production (Fig. 1b), but its overexpression decreased ROS (Fig. 1c). Although only cellular ATP was measured in this study, ROS-induced cell damage may have caused an increase in extracellular ATP, possibly affecting IL-1ra expression via P2X7R. Since the lack of P2X7R significantly reduces OXPHOS [44], the possible involvement of P2X7R in the MNSFβ knockdown-triggered metabolic changes requires investigation.

Our evaluation of the effects of MNSFβ on the regulation of glucose metabolism in murine peritoneal macrophages, which are not cancer cells, revealed no changes in lactate secretion, glucose consumption, or ROS production (Fig. 5c, 5d, and 5e). Notably, HIF-1α expression in peritoneal macrophages remained at a low level in the unstimulated state (Fig. 5b). These results suggest HIF-1α mediation of these MNSFβ-induced metabolic changes at least in Raw264.7 cells. The MNSFβ

knockdown-triggered changes may have been difficult to observe in unstimulated peritoneal macrophages because these cells primarily depend on OXPHOS for ATP production. In macrophages, LPS promotes the glycolytic pathway. The MNSFβ knockdown-triggered reduction in LPS-stimulated HIF-1α protein expression in peritoneal macrophages suggests that MNSFβ can regulate the glycolytic pathway in LPS-stimulated peritoneal macrophages. The present study implicates MNSFβ in glucose metabolism and inflammatory responses. As the effect of MNSFβ on glycolysis and mitochondrial metabolism is a new finding in the regulation of glucose metabolism, MNSFβ can be a potential target for the treatment of diseases, such as cancer, that involve metabolic changes due to HIF-1α activation. MNSFβ also alters cytokine production pattern, suggesting its involvement in inflammatory processes through HIF-1α signaling. This may help in the elucidation of new mechanisms in inflammatory diseases. Detailed molecular mechanisms of how MNSFβ specifically regulates HIF-1α and how this regulation affects metabolic pathways and cytokine productions might require further elucidation. Overall, MNSFβ may be an important ubiquitin-like protein that regulates multiple functions of macrophages.

The study primarily used the Raw264.7 cell line, which may not completely represent the behavior of human macrophages. Thus, caution should be exercised when extrapolating these results to humans. Moreover, experiments using human macrophages are needed to investigate the possibility of clinical application.

Statements and declarations

Funding: This study was supported by a grant-in aid for scientific research (C) to MN from the Ministry of Education, Culture, Sports, Science and Technology of Japan.

Conflict of interest: The authors declare no competing interests.

Ethics approval: All animal experiments (IZ3-55) were approved and performed according to the guidelines of the Animal Care Committee of Shimane University.

Author contributions

MN and MK designed the study. MK and KY conducted the experiments and MK performed the statistical analysis. MN and MK wrote the manuscript. All authors have read and approved the published version of the manuscript.

Acknowledgements

This work was supported by the Integrated Center for Mass Spectrometry, Graduate School of Medicine, Kobe University for metabolome analysis.

References

1. Nakamura M, Xavier RM, Tanigawa Y (1996) Ubiquitin-like moiety of the monoclonal nonspecific suppressor factor beta is responsible for its activity. J Immunol 156:532-8
2. Nakamura M, Xavier RM, Tsunematsu T, Tanigawa Y (1995) Molecular cloning and characterization of a cDNA encoding monoclonal nonspecific suppressor factor. Proc Natl Acad Sci U S A 92:3463-7
3. Nakamura M, Shimosaki S (2009) The ubiquitin-like protein monoclonal nonspecific suppressor factor beta conjugates to endophilin II and regulates phagocytosis. FEBS Journal 276:6355-63. https://doi.org/10.1111/j.1742-4658.2009.07348.x
4. Nakamura M, Watanabe N (2010) Ubiquitin-like protein MNSFβ/endophilin II complex regulates Dectin-1-mediated phagocytosis and inflammatory responses in macrophages. Biochem Biophys Res Commun 401:257-61. https://doi.org/10.1016/j.bbrc.2010.09.045
5. Watanabe J, Nakagawa M, Watanabe N, Nakamura M (2013) Ubiquitin-like protein MNSFβ covalently binds to Bcl-G and enhances lipopolysaccharide/interferon γ-induced apoptosis in macrophages. FEBS Journal 280:1281-93. https://doi.org/10.1111/febs.12120
6. Nakamura M, Yamasaki K, Kono M (2023) Ubiquitin-like protein MNSFβ regulates glycolysis and promotes cell proliferation with HSC70 assistance. Biochem Biophys Rep 33:101414. https://doi.org/10.1016/j.bbrep.2022.101414
7. Ke Q, Costa M (2006) Hypoxia-inducible factor-1 (HIF-1). Mol Pharmacol 70:1469-80. https://doi.org/10.1124/mol.106.027029
8. Masoud GN, Li W (2015) HIF-1α pathway: Role, regulation and intervention for cancer therapy. Acta Pharm Sin B 5:378-89. https://doi.org/10.1016/j.apsb.2015.05.007
9. Rani S, Roy S, Singh M, Kaithwas G (2022) Regulation of transactivation at C-TAD Domain of HIF-1α by factor-inhibiting HIF-1α (FIH-1): A potential target for therapeutic intervention in cancer. Oxid Med Cell Longev 2022:2407223. https://doi.org/10.1155/2022/2407223
10. Li ZL, Wang B, Lv LL, Tang TT, Wen Y, Cao JY, Zhu XX, Feng ST, Crowley SD, Liu BC (2021) FIH-1-modulated HIF-1α C-TAD promotes acute kidney injury to chronic kidney disease progression via regulating KLF5 signaling. Acta Pharmacol Sin. 42:2106-19. https://doi.org/10.1038/s41401-021-00617-4
11. Chen Q, Yang B, Liu X, Zhang XD, Zhang L, Liu T (2022) Histone acetyltransferases CBP/p300 in tumorigenesis and CBP/p300 inhibitors as promising novel anticancer agents. Theranostics 12:4935-48. https://doi.org/10.7150/thno.73223
12. Kiani AA, Elyasi H, Ghoreyshi S, Nouri N, Safarzadeh A, Nafari A (2021) Study on hypoxia-inducible factor and its roles in immune system. Immunol Med 44:223-36. https://doi.org/10.1080/25785826.2021.1910187

13. de Heer EC, Jalving M, Harris AL (2020) HIFs, angiogenesis, and metabolism: Elusive enemies in breast cancer. J Clin Invest 130:5074-87. https://doi.org/10.1172/JCI137552
14. Domènech M, Hernández A, Plaja A, Martínez-Balibrea E, Balañà C (2021) Hypoxia: The cornerstone of glioblastoma. Int J Mol Sci 22:12608. https://doi.org/10.3390/ijms222212608
15. Hoefflin R, Harlander S, Schäfer S, Metzger P, Kuo F, Schönenberger D, Adlesic M, Peighambari A, Seidel P, Chen C-Y, Consenza-Contreras M, Jud A, Lahrmann B, Grabe N, Heide D, Uhl FM, Chan TA, Duyster J, Zeiser R, Schell C, Heikenwalder M, Schilling O, Hakimi AA, Boerries M, Frew IJ (2020) HIF-1α and HIF-2α differently regulate tumour development and inflammation of clear cell renal cell carcinoma in mice. Nat Commun 11:4111. https://doi.org/10.1038/s41467-020-17873-3
16. Shiratori R, Furuichi K, Yamaguchi M, Miyazaki N, Aoki H, Chibana H, Ito K, Aoki S (2019) Glycolytic suppression dramatically changes the intracellular metabolic profile of multiple cancer cell lines in a mitochondrial metabolism-dependent manner. Sci Rep 9:18699. https://doi.org/10.1038/s41598-019-55296-3
17. Le A, Cooper CR, Gouw AM, Dinavahi R, Maitra A, Deck LM, Royer RE, Vander Jagt DL, Semenza GL, Dang CV (2010) Inhibition of lactate dehydrogenase A induces oxidative stress and inhibits tumor progression. Proc Natl Acad Sci U S A 107:2037-42. https://doi.org/10.1073/pnas.0914433107
18. Lian G, Li X, Zhang L, Zhang Y, Sun L, Zhang X, Liu H, Pang Y, Kong W, Zhang T, Wang X, Jiang C (2019) Macrophage metabolic reprogramming aggravates aortic dissection through the HIF1α-ADAM17 pathway. EBioMedicine 49:291-304. https://doi.org/10.1016/j.ebiom.2019.09.041
19. Nagao A, Kobayashi M, Koyasu S, Chow CC, Harada H (2019) HIF-1-Dependent reprogramming of glucose metabolic pathway of cancer cells and its therapeutic significance. Int J Mol Sci 20:238. https://doi.org/10.3390/ijms20020238
20. Basheeruddin M, Qausain S (2024) Hypoxia-inducible factor 1-alpha (HIF-1alpha): An essential regulator in cellular metabolic control. Cureus 16:e63852. https://doi.org/10.7759/cureus.63852
21. Lequeux A, Noman MZ, Xiao M, Van Moer K, Hasmim M, Benoit A, Bosseler M, Viry E, Arakelian T, Berchem G, Chouaib S, Janji B (2021) Targeting HIF-1 alpha transcriptional activity drives cytotoxic immune effector cells into melanoma and improves combination immunotherapy. Oncogene 40:4725-35. https://doi.org/10.1038/s41388-021-01846-x
22. Cramer T, Yamanishi Y, Clausen BE, Förster I, Pawlinski R, Mackman N, Haase VH, Jaenisch R, Corr M, Nizet V, Firestein GS, Gerber HP, Ferrara N, Johnson RS (2003) HIF-1alpha is essential for myeloid cell-mediated inflammation. Cell 112:645-57. https://doi.org/10.1016/s0092-8674(03)00154-5

23. Marrocco A, Ortiz LA (2022) Role of metabolic reprogramming in pro-inflammatory cytokine secretion from LPS or silica-activated macrophages. Front Immunol 13:936167. https://doi.org/10.3389/fimmu.2022.936167
24. Storti P, Bolzoni M, Donofrio G, Airoldi I, Guasco D, Toscani D, Martella E, Lazzaretti M, Mancini C, Agnelli L, Patrene K, Maïga S, Franceschi V, Colla S, Anderson J, Neri A, Amiot M, Aversa F, Roodman GD, Giuliani N (2013) Hypoxia-inducible factor (HIF)-1α suppression in myeloma cells blocks tumoral growth in vivo inhibiting angiogenesis and bone destruction. Leukemia 27:1697-706. https://doi.org/10.1038/leu.2013.24
25. Bateman RM, Tokunaga C, Kareco T, Dorscheid DR, Walley KR (2007) Myocardial hypoxia-inducible HIF-1alpha, VEGF, and GLUT1 gene expression is associated with microvascular and ICAM-1 heterogeneity during endotoxemia. Am J Physiol Heart Circ Physiol 293:H448-56. https://doi.org/10.1152/ajpheart.00035.2007
26. Ting KKY, Yu P, Dow R, Floro E, Ibrahim H, Scipione CA, Hyduk SJ, Polenz CK, Zaslaver O, Karmaus PWF, Fessler MB, Röst HL, Ohh M, Tsai S, Winer DA, Woo M, Rocheleau J, Jongstra-Bilen J, Cybulsky MI (2023) Oxidized Low-Density Lipoprotein Accumulation Suppresses Glycolysis and Attenuates the Macrophage Inflammatory Response by Diverting Transcription from the HIF-1α to the Nrf2 Pathway. J Immunol 211:1561-77. https://doi.org/10.4049/jimmunol.2300293
27. Liu Y, Xu R, Gu H, Zhang E, Qu J, Cao W, Huang X, Yan H, He J, Cai Z (2021) Metabolic reprogramming in macrophage responses. Biomark Res 9:1. https://doi.org/10.1186/s40364-020-00251-y
28. Tang Q, Wu S, Zhao B, Li Z, Zhou Q, Yu Y, Yang X, Wang R, Wang X, Wu W, Wang S (2024) Reprogramming of glucose metabolism: The hallmark of malignant transformation and target for advanced diagnostics and treatments. Biomed Pharmacother 178:117257. https://doi.org/10.1016/j.biopha.2024.117257
29. Vaupel P, Multhoff G (2021) Revisiting the Warburg effect: Historical dogma versus current understanding. J Physiol 599:1745-57. https://doi.org/10.1113/JP278810
30. Erdem A, Marin S, Pereira-Martins DA, Cortés R, Cunningham A, Pruis MG, de Boer B, van den Heuvel FA, Geugien M, Wierenga AT, Brouwers-Vos AZ, Rego EM, Huls G, Cascante M, Schuringa JJ (2022) The glycolytic gatekeeper PDK1 defines different metabolic states between genetically distinct subtypes of human acute myeloid leukemia. Nat Commun 13:1105. https://doi.org/10.1038/s41467-022-28737-3
31. Ortega E, Rengachari S, Ibrahim Z, Hoghoughi N, Gaucher J, Holehouse AS, Khochbin S, Panne D (2018) Transcription factor dimerization activates the p300 acetyltransferase. Nature 562:538-44. https://doi.org/10.1038/s41586-018-0621-1

32. Nakamura M, Notsu K, Nakagawa M (2019) Heat shock protein 60 negatively regulates the biological functions of ubiquitin-like protein MNSFβ in macrophages. Mol Cell Biochem 456:29-39. https://doi.org/10.1007/s11010-018-3487-5
33. Martínez-Reyes I, Chandel NS (2020) Mitochondrial TCA cycle metabolites control physiology and disease. Nat Commun 11:102. https://doi.org/10.1038/s41467-019-13668-3
34. Li Z, Zhang H (2016) Reprogramming of glucose, fatty acid and amino acid metabolism for cancer progression. Cell Mol Life Sci 73:377-92. https://doi.org/10.1007/s00018-015-2070-4
35. Anderson NM, Mucka P, Kern JG, Feng H (2018) The emerging role and targetability of the TCA cycle in cancer metabolism. Protein Cell 9:216-37. https://doi.org/10.1007/s13238-017-0451-1
36. Talwar H, Bouhamdan M, Bauerfeld C, Talreja J, Aoidi R, Houde N, Charron J, Samavati L (2019) MEK2 negatively regulates lipopolysaccharide-mediated IL-1β production through HIF-1α expression. J Immunol 202:1815-25. https://doi.org/10.4049/jimmunol.1801477
37. Murugina NE, Budikhina AS, Dagil YA, Maximchik PV, Balyasova LS, Murugin VV, Melnikov MV, Sharova VS, Nikolaeva AM, Chkadua GZ, Pinegin BV, Pashenkov MV (2020) Glycolytic reprogramming of macrophages activated by NOD1 and TLR4 agonists: No association with proinflammatory cytokine production in normoxia. J Biol Chem 295:3099-114. https://doi.org/10.1074/jbc.RA119.010589
38. Uehara I, Kajita M, Tanimura A, Hida S, Onda M, Naito Z, Taki S, Tanaka N (2022) 2-deoxy-d-glucose induces deglycosylation of proinflammatory cytokine receptors and strongly reduces immunological responses in mouse models of inflammation. Pharmacol Res Perspect 10:e00940. https://doi.org/10.1002/prp2.940
39. Zhu N, Mealka M, Mitchel S, Milani C, Acuña LM, Rogers E, Lahana AN, Huxford T (2023) X-ray crystallographic study of preferred spacing by the NF-κB p50 homodimer on κB DNA. Biomolecules 13:1310. https://doi.org/10.3390/biom13091310
40. Zhen X-X, Yang L, Gu Y, Yang Q, Gu W-W, He Y-P, Wang Y-L, Wang J (2021) MNSFβ regulates TNFα production by interacting with RC3H1 in human macrophages, and dysfunction of MNSFβ in decidual macrophages is associated with recurrent pregnancy loss. Front Immunol 12:691908. https://doi.org/10.3389/fimmu.2021.691908
41. Nakamura M, Omura S (2008) Quercetin regulates the inhibitory effect of monoclonal non-specific suppressor factor beta on tumor necrosis factor-alpha production in LPS-stimulated macrophages. Biosci Biotechnol Biochem 72:1915-20. https://doi.org/10.1271/bbb.80167
42. Wilson HL, Francis SE, Dower SK, Crossman DC (2004) Secretion of intracellular IL-1 receptor antagonist (type 1) is dependent on P2X7 receptor activation. J Immunol 173:1202-8. https://doi.org/10.4049/jimmunol.173.2.1202
43. Vultaggio-Poma V, Sarti AC, Di Virgilio F (2020) Extracellular ATP: A feasible target for cancer therapy. Cells 9:2496. https://doi.org/10.3390/cells9112496

44. Sarti AC, Vultaggio-Poma V, Falzoni S, Missiroli S, Giuliani AL, Boldrini P, Bonora M, Faita F, Di Lascio N, Kusmic C, Solini A, Novello S, Morari M, Rossato M, Wieckowski MR, Giorgi C, Pinton P, Di Virgilio F (2021) Mitochondrial P2X7 receptor localization modulates energy metabolism enhancing physical performance. Function (Oxf) 2:zqab005. https://doi.org/10.1093/function/zqab005

Table 1　Metabolome analysis

Raw264.7 cells were treated with siRNAs for 48 h and metabolites were detected by GC/MS.

Metabolite name	MNSFβ siRNA/Control siRNA	Metabolite name	MNSFβ siRNA/Control siRNA
Coniferyl alcohol	8.020	α-ketoglutarate	0.706
GABA	7.347	Succinate	0.682
2,3-Bisphospho-glycerate	2.348	Threonine	0.646
Sorbitol 6-phosphate	1.797	Mannitol	0.639
Serine	1.569	Cadaverine	0.600
Gluconic acid	1.567	beta-Alanine	0.593
Elaidic acid	1.494	Hypotaurine	0.586
Stearic acid	1.312	Alanine	0.586
Ethanolamine	1.283	Pyruvate	0.568
Glucosamine 6-phosphate	1.261	Terephthalic acid	0.556
Palmitoleic acid	1.139	Glycine	0.554
N-Methylethanolamine	1.063	Norleucine	0.544
Aspartate	1.062	Phenylalanine	0.537
n-Butylamine	1.057	Glycerol	0.531
Oxalic acid	0.991	trans-4-Hydroxyproline	0.528
Glutamate	0.911	Urea	0.509
Malate	0.858	Pyroglutamate	0.506
Inositol	0.837	Pyrophosphoric acid	0.494
2-Hydroxypyridine	0.836	Leucine	0.466
Oxamic acid	0.830	Valine	0.447
2-Aminoisobutyrate	0.815	Sorbose	0.428
n-Propylamine	0.800	Isoleucine	0.424
beta-Hydroxybutyrate	0.773	Citrate	0.416
1,5-Anhydro-D-glucitol	0.770	Proline	0.383
Fumarate	0.721	Lactate	0.326
Tagatose	0.711	Galactose	0.289

Figures

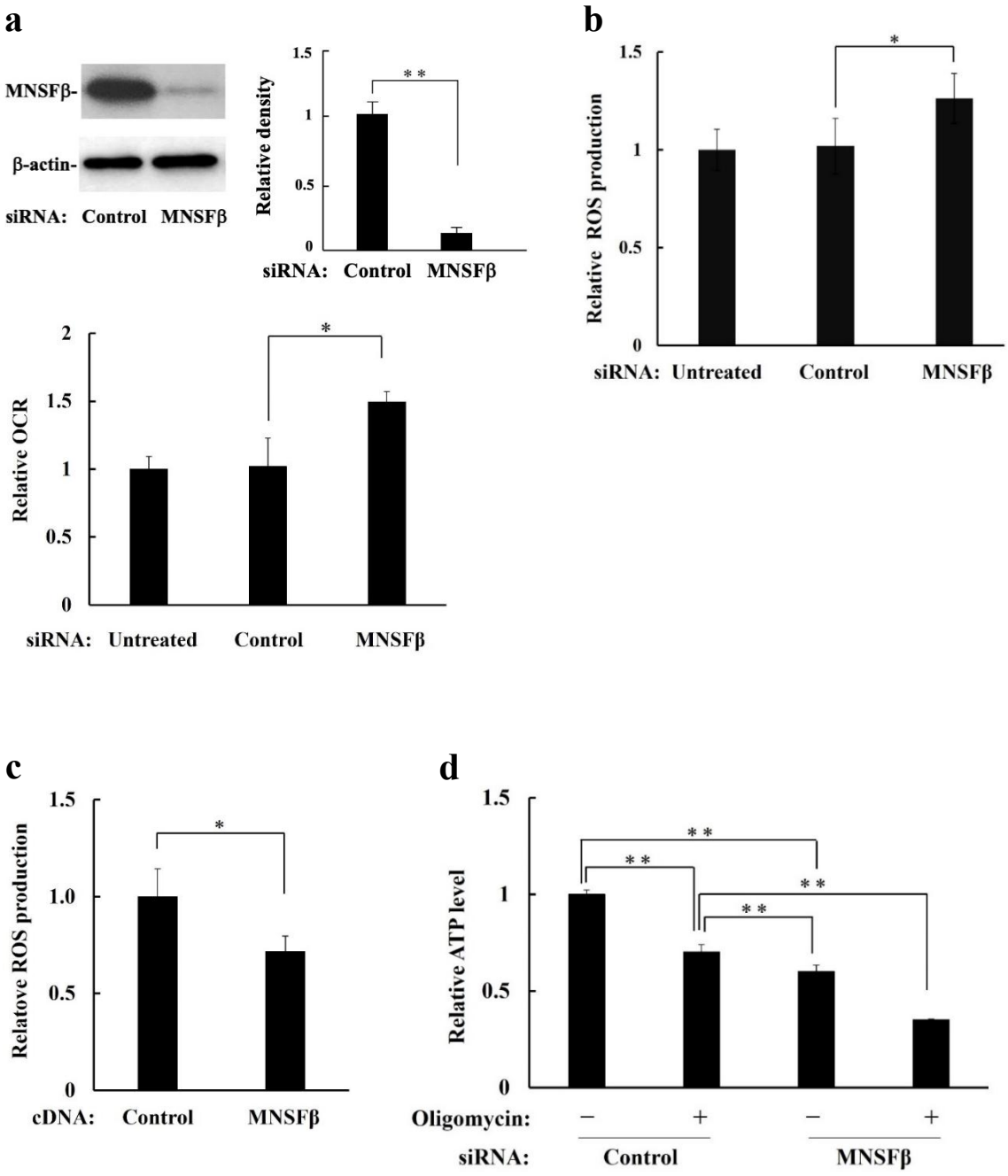

Fig. 1. MNSFβ shifts ATP production from glycolysis to oxidative phosphorylation

(a) Raw264.7 (1.0×10^4 cells/well) were transfected with siRNAs for 48 h, and OCR was measured using an Extracellular OCR Plate Assay Kit as described in Materials and methods section. ROS production of Raw264.7 (2.0×10^4 cells/well) transfected with siRNAs for 48 h **(b)** and cDNAs for 18 h **(c)** was measured as described under Materials and methods. **(d)** Raw264.7 cells (1.0×10^4 cells

per well) were transfected with siRNAs for 48 h, cells were stimulated with 1 μM oligomycin for 1 h. ATP was detected as described in the Materials and methods section. MNSFβ siRNA increased the oxygen consumption rate and ROS production but decreased ATP levels. The data are presented as the mean ± SD from three independent experiments (n=3). $^{**}P < 0.01$, $^{*}P < 0.05$.

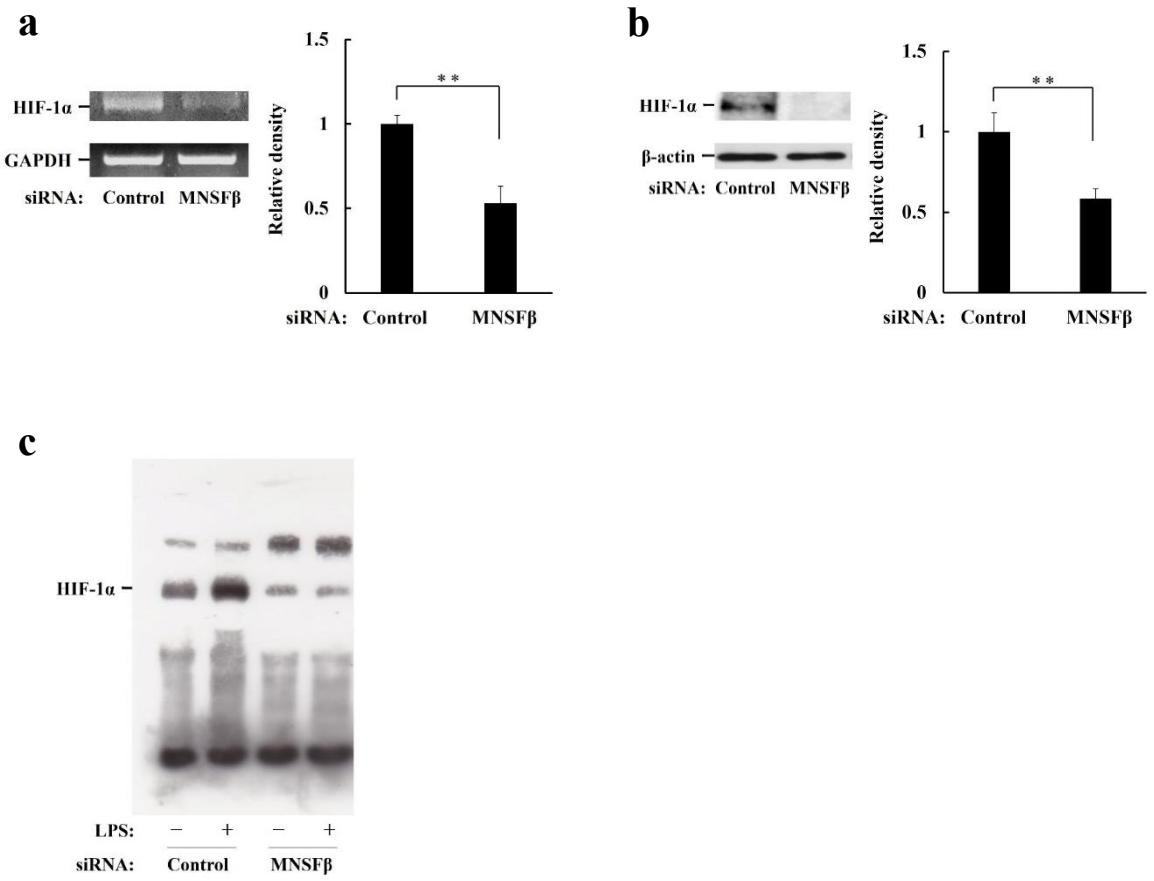

Fig. 2. MNSFβ regulates HIF-1α mRNA and protein expression in Raw264.7 cells.

Raw264.7 cells (1.0×10^5 cells per well) were transfected with MNSFβ siRNA for 48 h, and HIF-1α mRNA **(a)** and protein **(b)** expression were analyzed by RT-PCR and western blotting, respectively. **(c)** Raw264.7 cells (1.0×10^6 cells per well) were treated with siRNA for 48 h. The DNA binding activity of HIF-1α was evaluated by EMSA, as described in the Materials and methods section. The cells were stimulated with 1 μg/ml LPS for 24 h after 48 h transfection, and nuclear extracts were prepared. MNSFβ siRNA treatment decreased HIF-1α expression and DNA interaction. The data are presented as the mean ± SD from three independent experiments (n=3). $^{**}P < 0.01$.

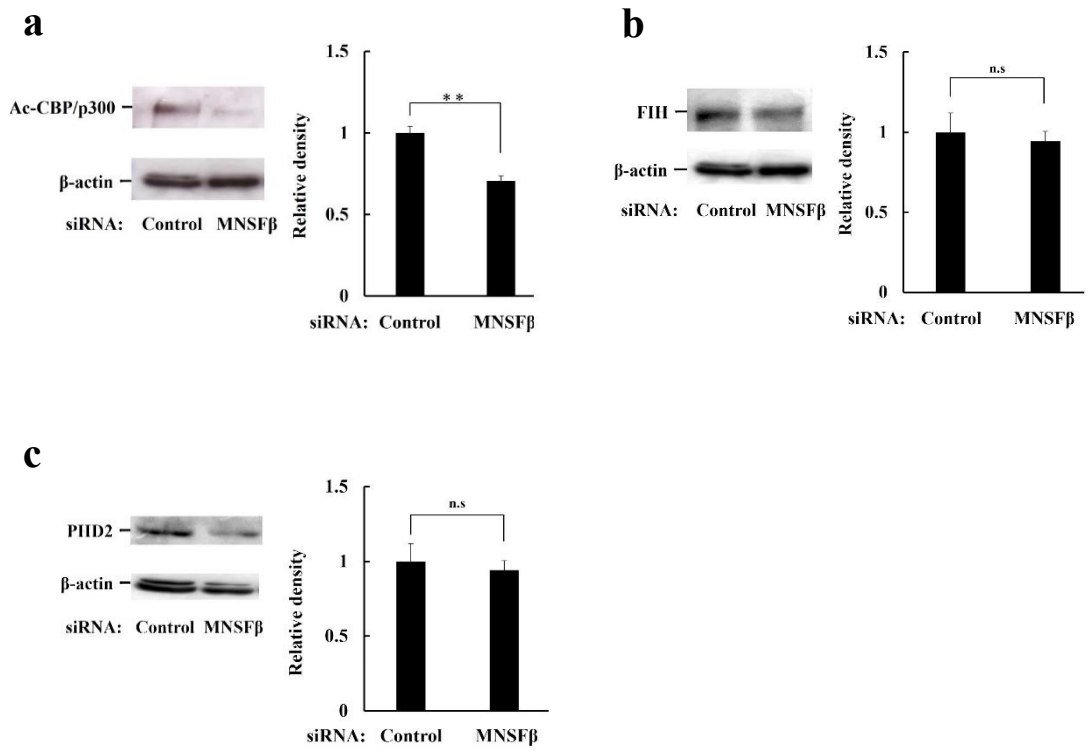

Fig. 3. MNSFβ siRNA decreases acetyl-CBP/p300 expression in Raw264.7 cells.

Raw264.7 cells (1.0×10^5 cells per well) were transfected with siRNA for 48 h, acetyl-p300/CBP **(a)**, FIH **(b)**, and PHD2 **(c)** expression were analyzed by western blotting with each specific antibody. MNSFβ siRNA treatment reduced acetyl-CBP/p300 expression without altering that of FIH and PHD2. The data are presented as the mean ± SD from three independent experiments (n=3). $^{**}P < 0.01$.

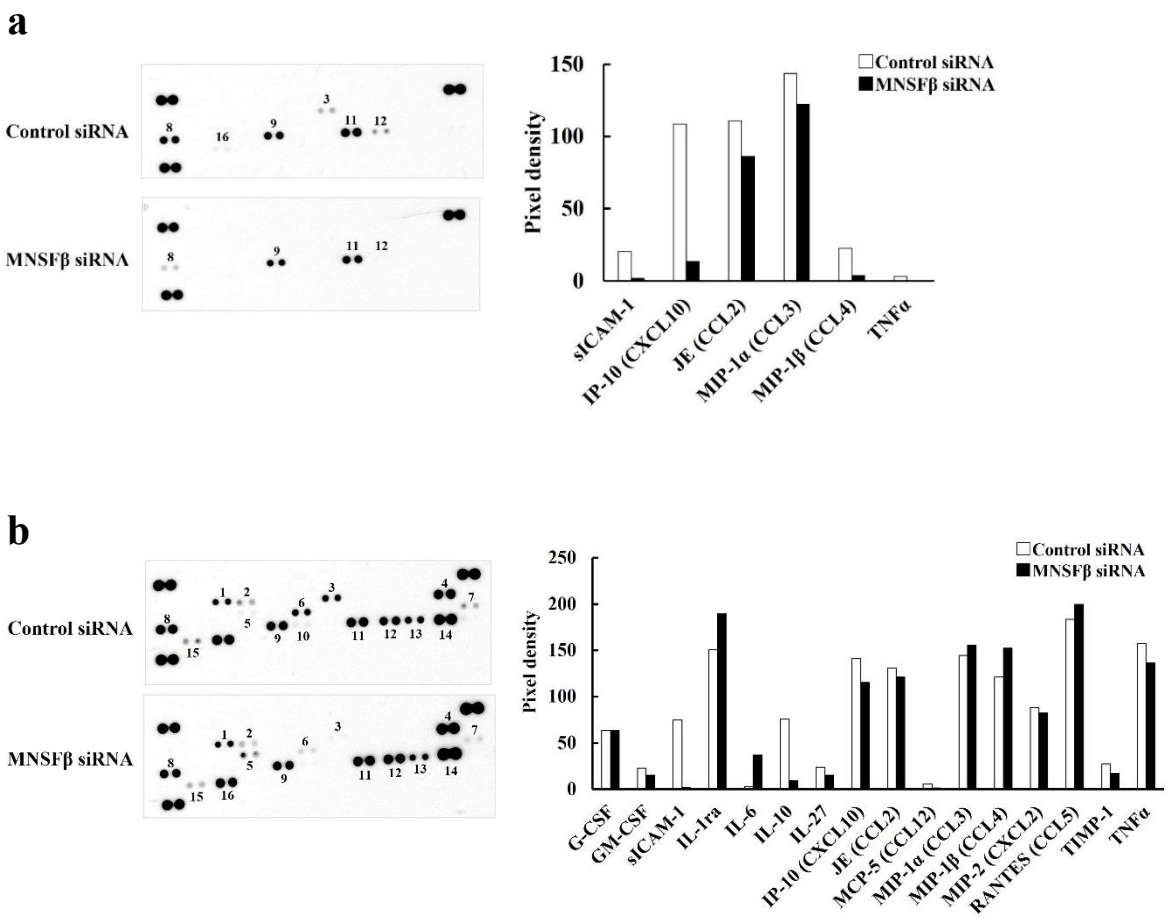

Fig. 4. MNSFβ changes cytokine production patterns.

Raw264.7 cells (1.0×10^5 cells per well) were treated with siRNA for 48 h and either untreated (**a**) or treated with 1 μg/ml LPS for 24 h (**b**). Cytokines in the culture supernatants were detected. 1, G-CSF; 2, GM-CSF; 3, sICAN-1; 4, IL-1ra; 5, IL-6; 6, IL-10; 7, IL-27; 8, IP-10 (CXCL10); 9, JE (CCL2); 10, MCP-5 (CCL12); 11, MIP-1α (CCL3); 12, MIP-1β(CCL4); 13, MIP-2 (CXCL2);14, RANTES (CCL5); 15, TIMP-1; 16, TNFα. Representative data are shown (n=2).

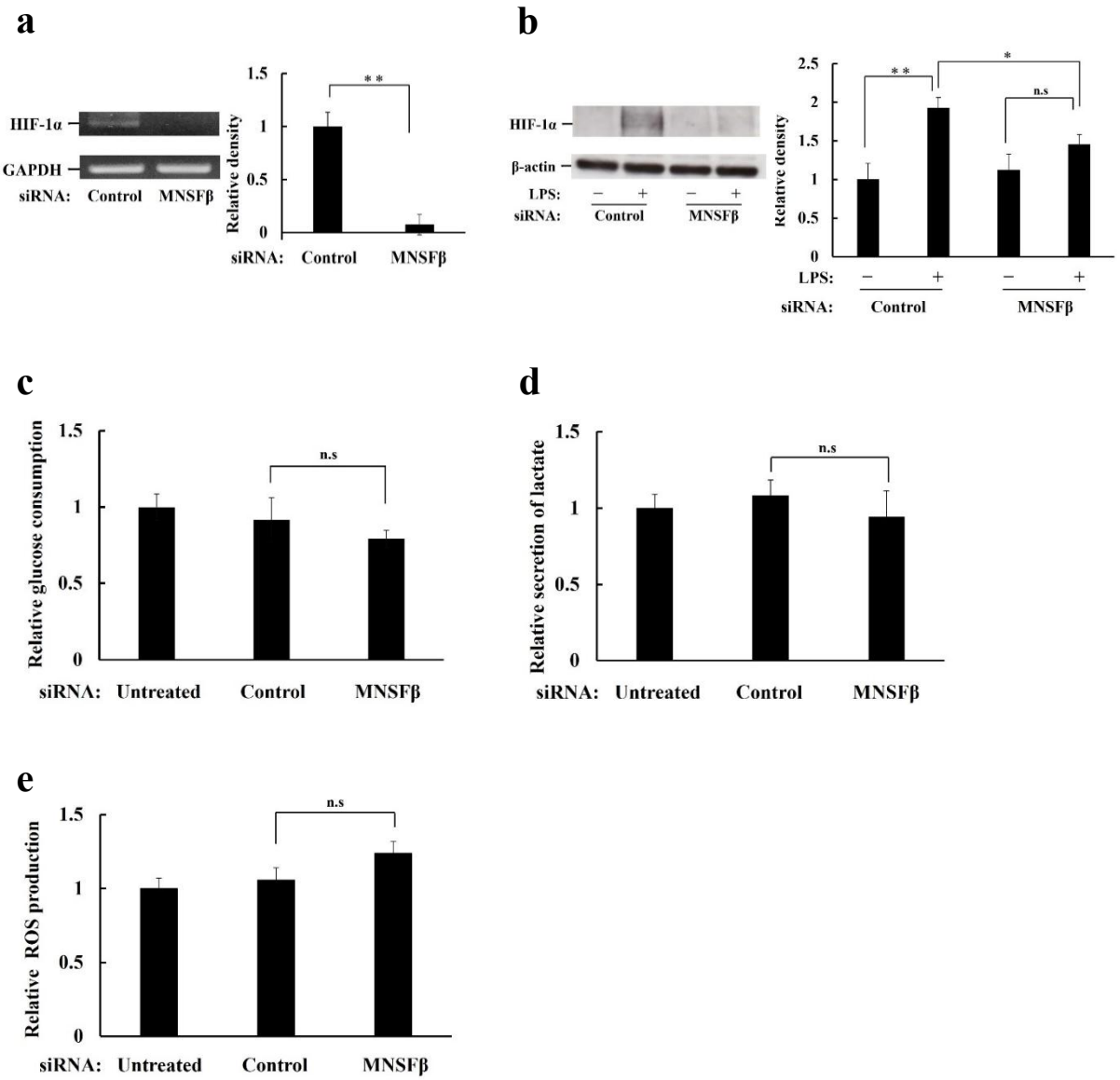

Fig. 5. MNSFβ regulates HIF-1α expression in murine peritoneal macrophages.

Peritoneal macrophages (1.0×10^5 cells per well) were transfected with siRNAs for 48 h and stimulated with LPS (1 μg/ml) for 24 h. MNSFβ mRNA **(a)** and protein **(b)** expression were analyzed by RT-PCR and western blotting, respectively. After 48 h transfection of peritoneal macrophages (2.0×10^5 cells per well) with siRNAs, glucose **(c)** and lactate **(d)** in the culture supernatant were detected. Peritoneal macrophages (2.0×10^4 cells per well) were treated with siRNA for 48 h and ROS production **(e)** were detected. Cells treated with MNSFβ siRNA showed no difference in glucose and lactate levels in the culture supernatant or in ROS production. Data are presented as the mean ± SD from three independent experiments (n=3). $*P < 0.05$, $**P < 0.01$.